Break junctions for molecular electronics using electromigration

Semester work done in the group of Prof. Dr. Wallraff A. at ETHZ
François Bianco

September 7, 2007

Contents

1 Introduction **1**
1.1 Goals 1
1.2 Electromigration 2
1.2.1 Description 2
1.3 Diffusion effects 4
1.4 The role of Joule heating 4
1.5 Quantization of the conductance 7
1.6 Breaking phases 9

2 Experimental setup **11**
2.1 Method 11
2.1.1 Feedback Algorithm 11
2.1.2 Four point measurements 12
2.1.3 Scanning-electron-microscope (SEM) 12
2.2 Device fabrication 14
2.2.1 Photolithography 15
2.2.2 Electron beam lithography 15
2.3 Sample Characterization 15
2.3.1 Device overview 17
2.3.2 Wire size 17

3 Results **19**
3.1 Discretised Conductance 19
3.2 Electromigration process 20
3.3 Gap size 22
3.4 Critical Power 23
3.5 Feedback Algorithm 26

4 Outlook **29**

5 Conclusion **30**
5.1 Acknowledgements 30

A Encountered problems **31**
A.1 Electrostatic 31
A.2 Fabrication 31

Abstract

During the last decades the exponential increase of the transistors number per chip has been following the empirical Moore's law, which states that this number double every 18 months. This increase has been followed by the reduction of the transistors size, which will soon reach physical limits. It is then probable that in a near future, new technologies like molecular electronics became the next step of (quantum) electronics. The key idea of molecular electronics is to connect single molecule to electrodes in order to build transistors or passive electronics components. At the current stage of research we are limited by our ability to build small enough electrodes.

One of the possible way to build such nanometer-spaced electrodes is to use electromigration, which is the ion mass flow when a high current density flows through a wire. In this work we present measurements of 30 electromigrated gold nanowires. We control the electromigration with a feedback algorithm to avoid a runaway of the process, our approach gives yields of more than 20% for junctions below 10 nm gap size. Our feedback is able to control electromigration and to produce junctions with very small gap sizes, but need to be fine tuned in order to increase its success yields. We also do a comparison of the breaking process with the simple Joule heating model, this one shows a large standard deviation, but this could be due to many issues, which we will discuss.

Chapter 1

Introduction

The idea of molecular electronics is to use single molecule as building blocks for passive and active electronics components, this could allow to reach quantum effects giving one the possibility to build quantum electronics.

To contact single molecules, two wires with nanometre spacing are required. This can be achieved by different methods (STM or AFM manipulation [16] [17] [18], mechanical [14] [6] or electromigrated break junction [8] [9]). Our chosen method is the electromigration of a nano wire. A high current density in a wire will produce mass flow by momentum transfer from electrons to ions. In a nanowire this will lead to a thinning and eventual breaking of the wire, creating the nanospaced electrodes required.

In this chapter a description of the electromigration (EM) is given, furthermore we present the role of Joule heating for EM and its link to the critical power needed to migrate a wire. In the next parts we derive the quantization of conductance and explain the different steps occurring during the breaking process.

1.1 Goals

The long term objective of this work is building molecular based electronics. The first problem arising is the small size of the electrodes needed to integrate a molecule into an electronic circuit, and it was the goal of this semester-work to try a reproducible way of creating such nanometer spaced electrodes. This distance is far beyond the resolution of common photolithographic techniques, thus different fabrication process is needed. We chose to use electromigration to create very small gaps in gold nanowires.

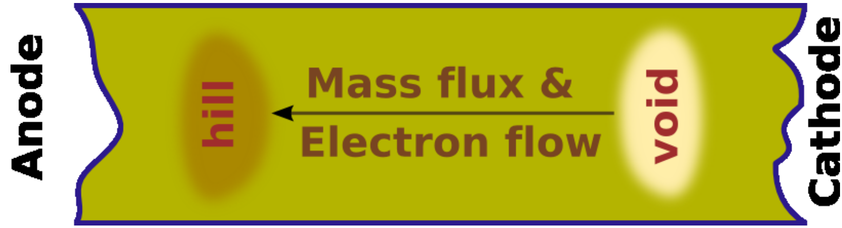

Figure 1.1: Schematic view of EM. The ion mass flux is driven by the electrical current through momentum transfer from the moving electrons to the ions. The displacement of the ions creates a void at one point, and a hill at the other side of the migration zone.

1.2 Electromigration

1.2.1 Description

Electromigration (EM) is a failure mechanism in electronics due to a mass flux of the metal ions driven by a high electrical current density (Fig. 1.1). There are two types of failure: an open circuit if all the atoms are removed at a point in a wire, or a short circuit if some atoms build a new connection, called whisker, with a neighboring wire.

This effect was discovered more than 100 years ago, but has been of practical interest only since the late 60s when people began to design electronics [19]. At this time James R. Black [1] derived his important equation describing the mean time to failure in a semiconductor circuit due to electromigration. Nowadays avoiding electromigration plays an important role in electronic design because of the constantly decreasing wire cross sections and thus increasing current densities.

The metal ions are distributed in a lattice created by their repulsion forces and the binding forces of their surrounding electron cloud. This lattice describes potential wells in which the atoms oscillate. If an atom acquires a higher energy than the potential barrier of its well, it could flow away or fall back to its position. This process does not cause any mass flux because its direction is randomly distributed [2]. Electromigration will occur when some of the momentum of the moving electrons is transfered to activated ions.

If a current is present in a conductor the metal ions will feel two forces: one due to the presence of the electric field $\vec{F}_e$ and a second one due to the electron movement $\vec{F}_p$. The latter force is caused by momentum exchange between the electrons and the ions, this is the so-called *e*lectron wind (Fig. 1.2). The resulting force is

$$\vec{F} = \vec{F}_e - \vec{F}_p. \tag{1.1}$$

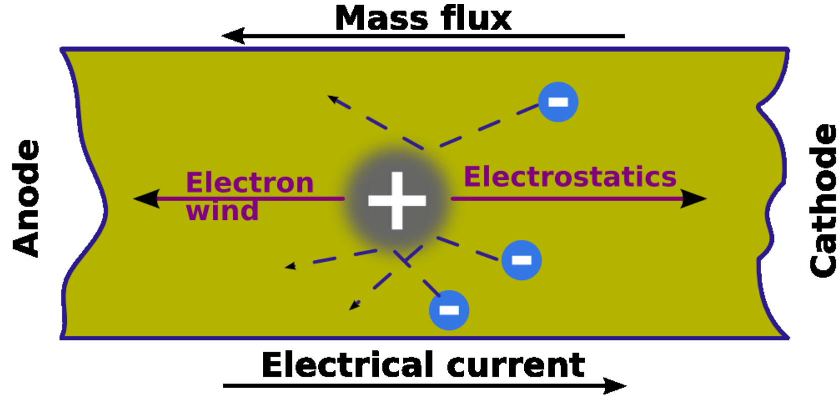

Figure 1.2: The two forces acting on the ion (+) which cause an ion mass flux (EM). One force on the ion is due to the electrostatic potential across the wire, the second force arises from the electrons (-) scattering on the metal ion (+) causing the so called electron wind.

In this equation we have already taken into account that the electron charge is negative, thus the two forces act in opposite directions. This force can be rewritten as

$$\vec{F} = Z^* e \vec{E} \tag{1.2}$$

where $\vec{E}$ is the electric field and $Z^* e$ the effective charge which describes the scattering cross section between the mobile electrons and the metal ions [2].

In order to give a full description of the electromigration process we need to use the theory of irreversible thermodynamics processes, in this part we follow the derivation of Trouwbrost M.L [3]. Thermodynamics yields the relations between the flux of the metal atoms J_m, the energy flux J_u, the electron particle flux J_e and the three potential gradients: the chemical potential μ, the electrostatic potential φ and the temperature gradient ∇T. Thus EM is described by

$$J_m = -L_{m,m} \nabla \left(\frac{\mu^m + Ze\varphi}{T} \right) - L_{m,e} \nabla \left(\frac{\mu^e - e\varphi}{T} \right) - L_{m,u} \frac{\nabla T}{T^2} \tag{1.3}$$

where Z is the ion charge, the $L_{m,*}$ are phenomenological constants proportional to the diffusion coefficient, and the μ's are the chemical potentials related to the electrons (^{e}) and ions (^{m}). We will neglect the temperature gradient, which causes only small effects over the size of the junction. Moreover we note that the effect of the chemical potential on the electrons is negligible compared to the electrostatic one, therefore we get

$$J_m = -\frac{1}{T} \left(L_{m,m} \nabla \left(\mu^m + Ze\varphi \right) - L_{m,e} e \nabla \varphi \right). \tag{1.4}$$

Then we use Ohm's law:$-\nabla\varphi = \rho j$ and rewrite the coefficient $L^* = L/T$ to arrive at:

$$J_m = -L^*_{m,m}(\nabla\mu^m - \underbrace{(Z - \frac{L_{m,e}}{L_{m,m}})}_{Z^*} e\rho j). \tag{1.5}$$

Z^* represents the effective charge, which is due to momentum transfer from the electrons to the ions. In normal cases Z^* is positive, so the resulting net force will be in the direction opposite to the electrical current.

1.3 Diffusion effects

It is also important to consider the effects of diffusion on the EM process. The diffusion coefficient D is a measure of the mobility of particles, which depends strongly on the temperature

$$D = D_0 e^{\frac{-E_A}{kT}}. \tag{1.6}$$

E_A represents the activation energy, only the atoms with an higher energy will contribute to diffusion.

Due to the symmetry in a perfect lattice there is rarely any diffusion, but a real material is composed of grains, which are small regions of perfect crystal structure with different orientation relative to each other. At the grain boundaries and at the surface the symmetry is broken, leaving the ions less bounded than at other points of the structure. Therefore the activation energy is smaller than within the lattice and the grain boundary is the principal location of diffusion. The lattice diffusion mechanism is less present but can appear at high local temperature when many ions are thermally excited [4]. The three locations for diffusion are therefore: at the grain boundaries, at the surface, or within the lattice structure itself (Fig.1.3).

It is also known that atomic rearrangement at the surface tends to release mechanical strain which occurs during the electromigration [11]. This surface reconstruction could be responsible for rebuilding a junction during the EM process.

1.4 The role of Joule heating

Joule heating is the process by which an electric current releases heat. Its name is related to James Prescott Joule who first described this effect. The heat production arises from collisions between the charge carriers driven by the applied electric field and the ions constituting the body of the conductor.

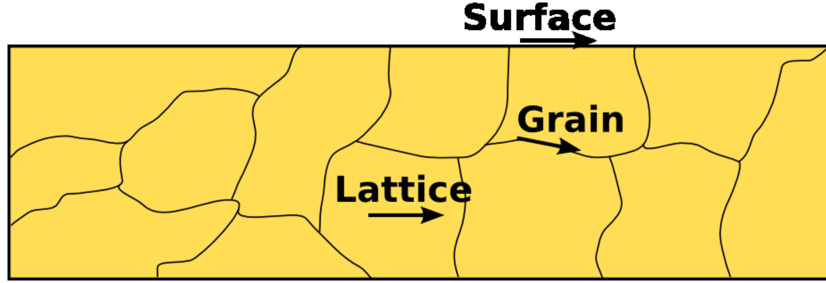

Figure 1.3: Diffusion, represented by arrows, is easier where the symmetry is broken, like at the surface and at the grain boundaries. The third diffusion location within the lattice is present only at high local temperature when many ions are thermally activated.

Hence this process converts the electrical energy supplied by the power source to thermal energy in the wire and the surrounding material.

We know that electromigration needs thermally activated ions to start, which more likely will be the case at the locations where the activation energy is small: at grain boundaries and at the surface of the wire. Moreover these locations have no symmetry and are therefore scattering electrons, increasing the local temperature by Joule heating.

As soon as the junctions shrink, the local current density increases and thus the heat production increases as well. There are two effects due to this increase of the local temperature: the diffusion coefficient grows, and the thermal vibrations of the lattice increase, which further accelerates the process. The phonons are responsible for inhomogeneities within the lattice structure which create new scattering centers for the moving electrons. Therefore the cross section of the electron-ion scattering becomes bigger. A schematic view of the whole mechanism is represented in figure 1.4.

As soon as the migration starts, the heat production increases if the voltage drop across the junction is not reduced. This heat can induce a local melting of the metal in the junction. The typical signature of melting is a large (> 200 nm) junction with rounded borders and small metal islands within the junction (Fig. 1.5).

We are now interested in finding the critical power needed to start the migration in the wire. Thus we write down the Joule heating equation which describes the relation between the dissipated power P, the current I and the resistance R_j:

$$P^* = R_j I^{*2} \tag{1.7}$$

where the stars denotes the critical current and power. Using Ohm's law one

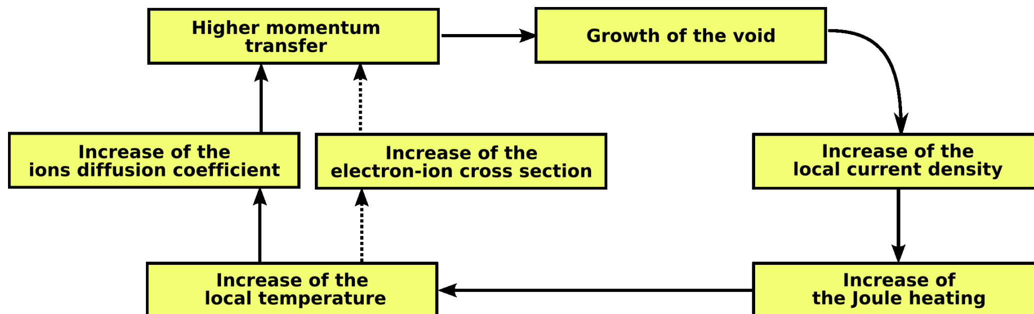

Figure 1.4: Schematic view of the breaking mechanism. As soon as it starts, the process accelerates itself by feedback effects (increase of the diffusion coefficient and scattering cross section) due to local Joule heating.

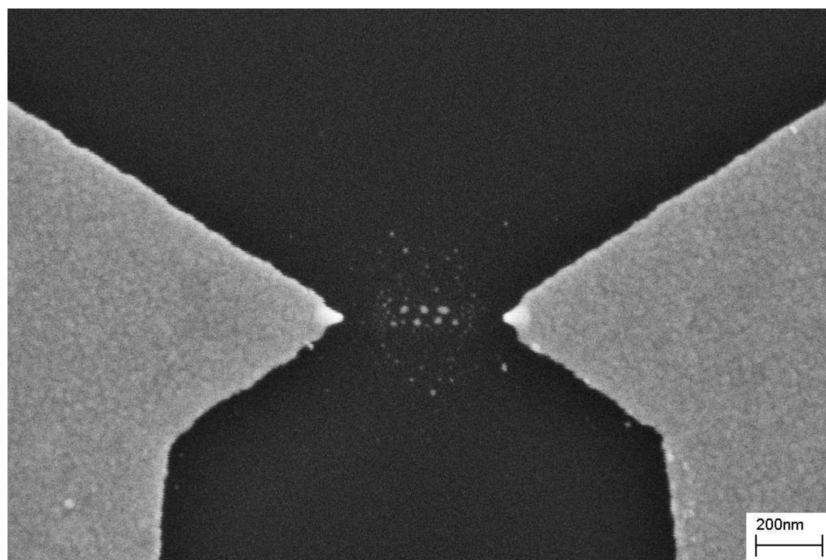

Figure 1.5: Zoom of a melted junction, where the heat production was too important. Small metal islands are present within the junction.

can derive a relation between the applied voltage $V*$ and the conductance:

$$P^* = R_j \frac{v^{*2}}{(R_s + R_j)^2}. \tag{1.8}$$

Solving for the voltage yields:

$$v^* = \sqrt{\frac{P^*}{G^2}\frac{1}{R_j}} = \sqrt{\frac{P^*}{G^2}\frac{1}{R_j + R_s - R_s}} = \sqrt{\frac{P^*}{G}\frac{1}{1 - GR_s}}. \tag{1.9}$$

This relation allows, if we know the relation between the voltage and the conductance $V(G)$, a fit of the critical power [8]. This model is valid for nanowires above a conductance of 2-3 mS. Below this value quantum effects not considered in the Joule heating model become important.

1.5 Quantization of the conductance

During the EM process the wire cross section reaches the size of the Fermi wavelength of electrons in the metal used. For this size the conductance no longer drops continuously but shows discrete steps.

First we will try to explain the quantization with a very simple model following the idea of Crowell B.W. [5]. In the second part we will use only quantum mechanical arguments to explain the presence of discrete steps.

Replacing a continuous current by a discrete number of electrons flowing results in:

$$I = \frac{\Delta Q}{\Delta t} = \frac{\Delta N e}{\Delta t} = \Delta N e \frac{v}{L} \tag{1.10}$$

where e is the electron charge, L the distance over which the electrons travel, and ΔN the number of electrons passing through the junction within the time Δt. We define V as the voltage across the wire, and then use the Ohm's law to find a relation for the conductance:

$$G = \frac{I}{V} = \frac{\Delta N e v}{LV}. \tag{1.11}$$

The effect of quantum mechanics is introduced by using the de Broglie wavelength of a particle in a box $\lambda = L/n$, with n an integer greater than zero, and the Heisenberg Uncertainty Principle $\Delta p \Delta x \leq h$, with h the Planck constant. Knowing that the momentum is given by $p = mv$ and that the uncertainty in the position for a wavepaket is equal to its wavelength, results in

$$mv\frac{L}{n} \leq h. \tag{1.12}$$

The Pauli Exclusion Principle states that no two electrons can be in the same quantum states, but there is a spin degeneracy of 2, giving us the relation $2n = \Delta N$. Inserting this relation in Eq. (1.12) and assuming the equality yields

$$\Delta N = \frac{2Lm\Delta v}{h}. \tag{1.13}$$

We rewrite the voltage drop as a change in the potential energy: $\Delta U = eV$ which is equal to a change in the kinetic energy $\Delta T = mv\Delta v$. Then if we insert the latest relation and the Eq. (1.13) into Eq. (1.11) for the conductance we find

$$G = \frac{2e^2}{h}. \tag{1.14}$$

This represents the conductance quantum $G_0 = 7.75 \cdot 10^{-5}$ S, which, multiplied by integer number, gives the possible quantized values for the conductance.

A better theoretical explanation can be derived by solving the Schrödinger equation. We follow a calculation of Ihn T. [15]:

$$i\hbar\delta_t\psi = H\psi \tag{1.15}$$

where H is the Hamiltonian for electrons in the wire. Considering a nanowire with infinite length in the y direction defines a translational invariant symmetry (Fig. 1.6). Therefore the wavefunction of the electron can be separated as

$$\psi_{n\vec{k}}(\vec{r}) = \chi_n(x,z)\frac{1}{\sqrt{L}}e^{ik_y y} \tag{1.16}$$

where χ_n is the solution in the plane of the wire and the exponential function is a plane wave with a norm L. The quantum number n is discrete and is given by the boundary conditions. The contribution of an electron in state (n, k_y) to the electrical current density is given by (we take $e > 0$):

$$\vec{j}_{nk_y} = -\frac{e\hbar}{2im^*}\left(\psi^*_{nk_y}(\vec{r})\nabla\psi_{nk_y}(\vec{r}) - \psi_{nk_y}(\vec{r})\nabla\psi^*_{nk_y}(\vec{r})\right) \tag{1.17}$$

where m^* is the effective mass due to the band structure in the metal. Inserting the wave function in Eq. (1.17) leads to

$$\vec{j}_{nk_y} = \underbrace{-e\frac{1}{L}|\chi_n(x,z)|^2}_{\rho}\underbrace{\frac{\hbar k_y}{m^*}\vec{e}_y}_{\vec{v}} \tag{1.18}$$

where ρ represents the charge carrier density and $\vec{v}$ the group velocity. To get the total current we have to sum over all the allowed k_y and n. If

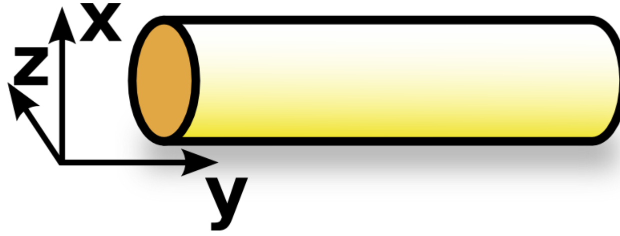

Figure 1.6: Schematic view of the wire

the cross section is reduced the boundary conditions change, and there are fever possible values of n below the Fermi energy in the wire. Therefore the number of electrons allowed within the junction by the Pauli Exclusion principle decreases in discrete steps as the junction shrinks. We know that the conductance is directly related to the number of electrons allowed to pass though the junction, explaining why the conductance should show plateaus at integer values.

1.6 Breaking phases

The breaking process in a junction starts from a normal bulk contact (Fig. 1.7 (a)), where the electron transport is diffusive. Then as the voltage increase the current increase linearly, as stated by the Ohm's law, but at a given voltage, depending on the cross section of the wire, the linear response is broken by the start of the electromigration process. At this point the wire cross section is much bigger than the wave length of the electrons, thus the measured conductance changes continuously because it is a mean over a lots of conductance channels. The electromigration reduces the wire cross section, and after some time its size will be in the scale of the Fermi wave length of the electrons, therefore the charge transport becomes ballistic.

This is visible in the conductance plots, which shows a transition around $20G_0$ from a continuously changing conductance to a regime in which the conductance changes in discrete steps. Some conductance steps are visible in the plot on the left of Fig. (1.7). When the conductance reaches approximately 1 G_0 the wire has only one quantum channel left, meaning that only one electron could flow at a time through the wire. At this point the wire could be made of a single or a chain of atoms (Fig. 1.7 (b) and (c)), but it is also possible that there are many atoms in a configuration allowing only one quantum channel. The final step is the breaking itself, after which a current flow is only possible by a tunnel process (Fig. 1.7 (d)) through the air or through the substrate surface. [8]

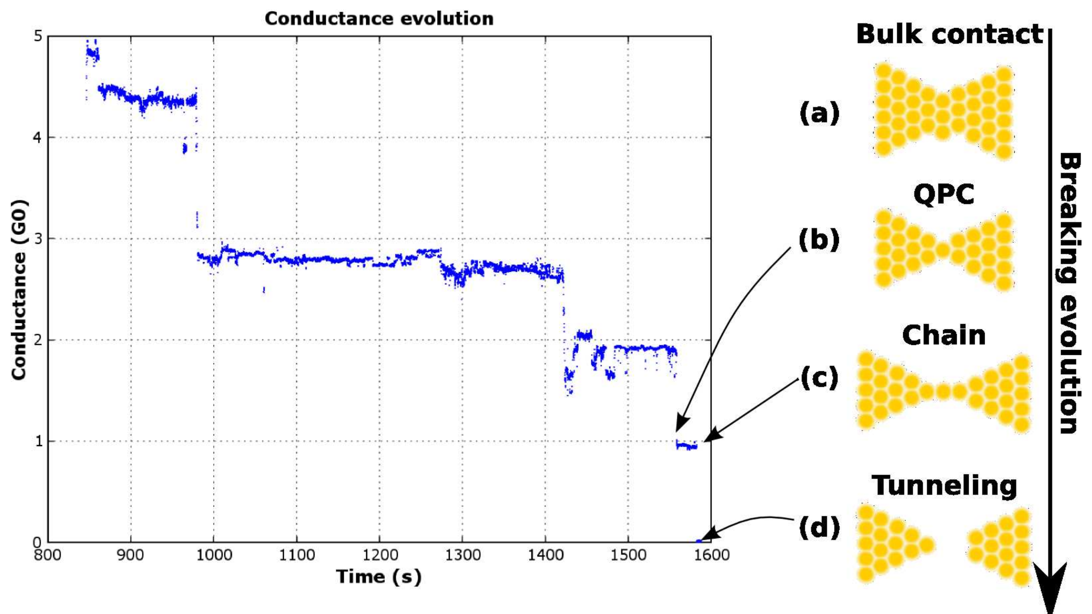

Figure 1.7: Detail of the breaking phases of a junction. At the beginning (a) the electron transport is diffusive, at around $20G_0$ the transport starts to show a ballistic behaviour, where the conductance is quantized. We say that the wire behaves like a quantum point contact (QPC) (b). On the last plateau at $1G_0$ the wire has only one quantum channel left, it could be a single atom or (b) or a chain of atom (c) but it could as well be many atoms in a configuration allowing only one electron channel. After breaking, a current flow is only possible by tunneling processes (d).

Chapter 2

Experimental setup

First we present the methods and the software used for the measurement of the junction EM. Then we explain the device fabrication and show an overview of the realized chips.

2.1 Method

To measure the EM of the junctions a four point measurement with a source-measure unit (SMU) *Keithley 2601* is used. The SMU is connected to a computer running a homemade software which controls the evolution of the process by different feedback mechanisms. After the migration, to determine gap sizes, pictures of the samples were taken with a scanning-electron-microscope.

2.1.1 Feedback Algorithm

To break the wire in a controlled fashion specialized software was written. The goal is to reach the last conductance plateau and to avoid a runaway of the EM. Different feedback mechanisms were implemented to control the electromigration of the wire. A flow chart of the feedback process is shown in Fig. (2.1).

The program applies voltage ramps and then controls the breaking using one of the two feedback mechanisms. Firstly new voltage value is set on the SMU, then the program starts a loop of measurements at constant voltage. The first feedback mechanism is related to the resistance, it computes the relative change of the resistance against a reference value stored before the loop started. Below a conductance of $15G_0$, a second feedback mechanism is used, this one checks the fluctuations of G/G_0, which are more representative than the resistance evolution at the end of the breaking process.

The two feedback mechanisms have two ways for detecting peaks. Either by counting the number of values outside of a given interval, and if this number reaches the fixed limit, the program steps down the voltage; or the second method is to average some measurements and to compute the relative change against the reference value stored at the beginning of the loop. Each time the voltage is set down, the program starts a the loop again with the lower voltage. In the other case, if there were no positive feedback detections, the voltage is increased and a new loop starts.

The software has two other security limits: a maximum voltage (300-400 mV) and maximum current (8-10 mA) depending on the stage of breaking. If one of those limits is reached, even before any changes in the junction occurs, the program starts a new voltage ramp from a lower voltage to prevent a possible runaway.

A third method was applied during the first measurements. This one computes the normalized breaking rate $\frac{1}{R}\frac{\partial R}{\partial t}$, and compared it to a given value to decide if it should reduce the voltage across the junction.

2.1.2 Four point measurements

The simplest layout for measuring a resistance is to use a voltage source and an amperemeter to measure the current (Fig. 2.2 a). The resistance is then given by the Ohm's law. This method has the disadvantage of including the lead resistance, the internal resistance of the voltage source and that of the amperemeter in the result:

$$R_{mes} = \frac{U}{I} = R_j + 2R_c + R_i + R_v \tag{2.1}$$

where R_j is wire resistance, R_c the contact resistance, R_i the internal resistance of the ampermeter and R_v the internal resistance of the voltage source.

To avoid this error the four point measurement technique was used. A current source delivers a constant current (independent of the voltage across the circuit) and we measure the voltage drop only across the junction with a voltmeter (Fig. 2.2 b). The internal resistance of the voltmeter has to be much higher than the measured resistance, such that all the current will go through the junction. Thus we can compute the junction resistance R_j using the Ohm's law. We notice that the internal resistance of the voltmeter can be actually a limitation for very high impedance measurement.

2.1.3 Scanning-electron-microscope (SEM)

The scanning electron microscope (SEM) is a type of electron microscope capable of producing nanometers-resolution images of a sample surface. In

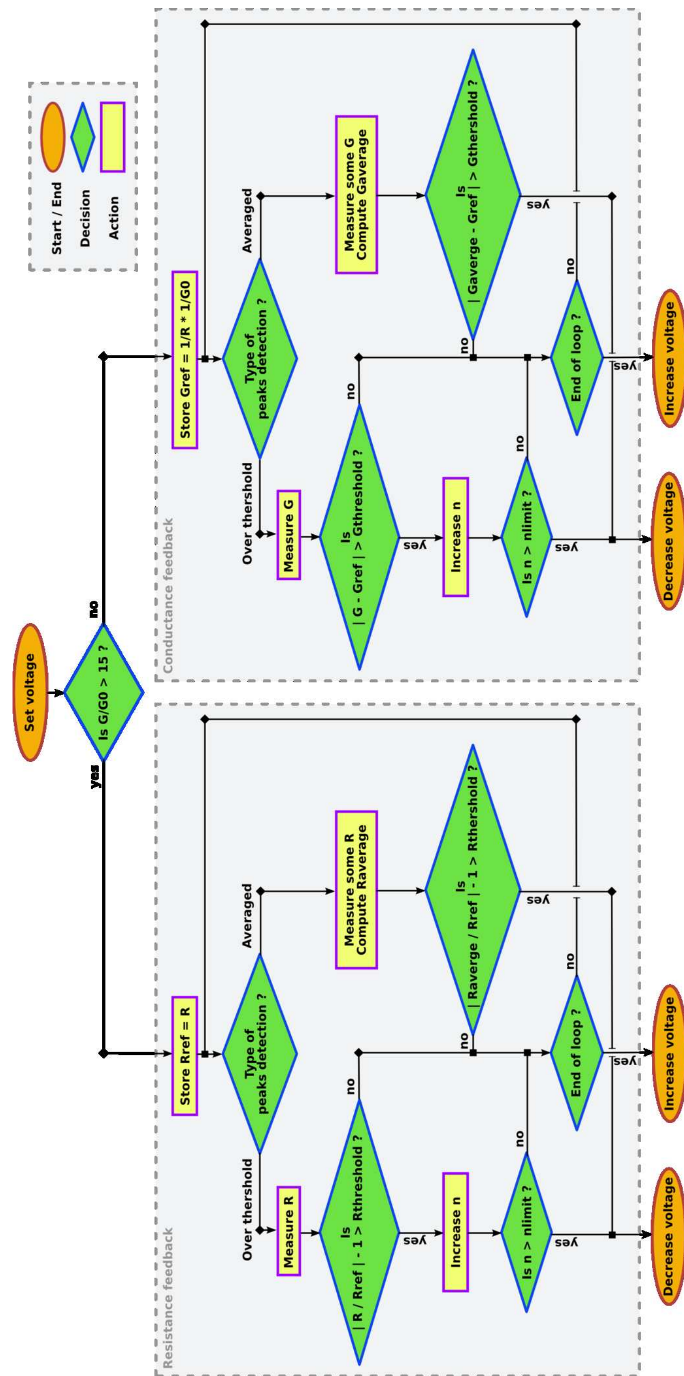

Figure 2.1: Feedback flow chart. The two feedbacks are visible. On the left the resistance feedback for conductance values above $15G_0$. On the right the conductance feedback used at the end of the breaking process (ie. below $15G_0$). When the program reaches the end of the chart it starts the process again.

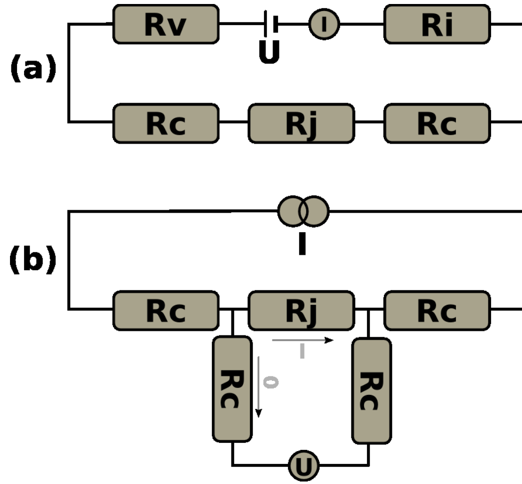

Figure 2.2: (a) Schematic of a two point measurement. The measurement includes all the resistances to the result. (b) Schematic of a four point measurement. This layout allows one to measure R_j without including the other resistances. In both (a) and (b) R_j is the junction resistance, R_c the contact and wiring resistance, R_i the internal resistance of the ampermeter, and R_v the internal resistance of the voltage source.

a typical SEM, electrons are emitted and accelerated in the direction of the sample. On the surface the electron beam interacts with the top of the surface, the electrons are scattered and lose energy or are absorbed. As a result electrons and electromagnetic fields are emitted from the surface, which can be detected in order to produce a picture of the sample [19]. All our pictures were produced with a *Zeiss ULTRA 55*.

2.2 Device fabrication

The breakjunctions were fabricated in FIRST, a clean room facility at ETH Zurich. Due to the small size of the junctions, bigger wires are necessary for the connection to the measurement instrumentation. A two step process is necessary for fabrication. Firstly the external wires are made by a standard photolithographic technique. Then, because the sizes are below the resolution of photolithography, the gold wires are defined using electron beam lithography.

2.2.1 Photolithography

Photolithography or optical lithography uses light to transfer a pattern from a shadowmask to a light-sensitive photoresist on the substrate. After the exposure, a series of chemical treatments reproduces this pattern on the material underneath the resist. The resolution is limited by the wavelength of the light according to:

$$F = k \cdot \frac{\lambda}{N_A} \tag{2.2}$$

where F is the minimum feature size, k is a coefficient that encapsulates process-related factors, typically $k \approx 0.5$, λ is the wavelength of light used, and N_A is the numerical aperture of the lens as seen from the wafer. The common resolution is between 1 μm to 500 nm in research facilities, but could go down, with special equipement, to 50 nm for the realisation of central processing unit (CPU).

2.2.2 Electron beam lithography

Electron beam lithography (EBL) uses, as the name suggests, a beam of electrons to create patterns on a surface. The use of electrons to draw a structure allows a higher resolution, because the wavelength of the electrons is smaller than for photons. The limit in resolution for EBL is about 20 nm [12], which is much smaller than for photolithography. The main disadvantage of this technique is that it is a sequential process, which increases the time needed to build a chip compared to common optical lithography, where the process simultaneously exposes each parts of the device. Writing the connection pads with EBL as well would increase the EBL time from less than hour to more than one day. This step was performed with a *Raith 150*.

2.3 Sample Characterization

Minimizing the serial resistance of the voltage probe wire was the main factor influencing chip design. There were two different photolitographic designs for the external wiring (Fig. 2.5 (a) and (b)), and two possible geometries for the junction: wire or bowtie, the second one was design to avoid many electromigration points along the junction. The different sizes are given below in section 2.3.2). The lead designs also varied as shown in figures 2.3 and 2.4, the second lead design simplify the connections to the measurement instrumentation.

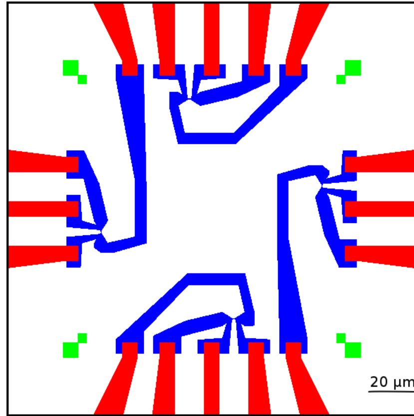

Figure 2.3: Schematic overview of the first lead design. A part of the external connectors is visible in the picture (red). The inside part shows the connection form the junctions to the bigger wires (blue). The green structures are drawn only for the alignment

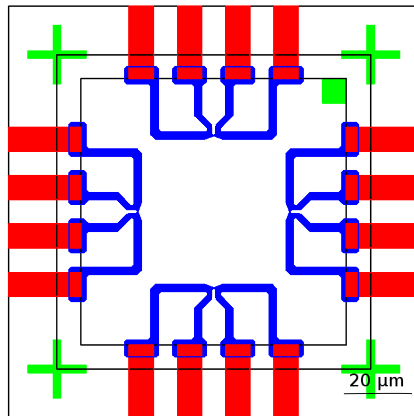

Figure 2.4: Schematic overview of a second lead design used. A part of the external connectors is visible in the picture (red). The inside part shows the connection form the junctions to the bigger wires (blue). The green arrows are drawn only for the alignment

2.3.1 Device overview

On each chip (5 mm) we realized four small devices (Fig. 2.5 (a) 100 μm) each with four junctions (100 nm), as shown in figure 2.5 (b). The figure 2.5 (c) shows the center of the structure, and a single junction is visible in 2.5 (d). All these pictures were taken with a SEM.

2.3.2 Wire size

The table below presents the different sizes of the wires.

Device	Geometry	Length (nm)	Width (nm)	Thickness (nm)
1 & 2	wire	500	70	30
3 & 4	wire	500	75	30
7 & 8	wire	400	80	30
02	bowtie	-	100	30

Table 2.1: Sizes and geometries of the measured devices.

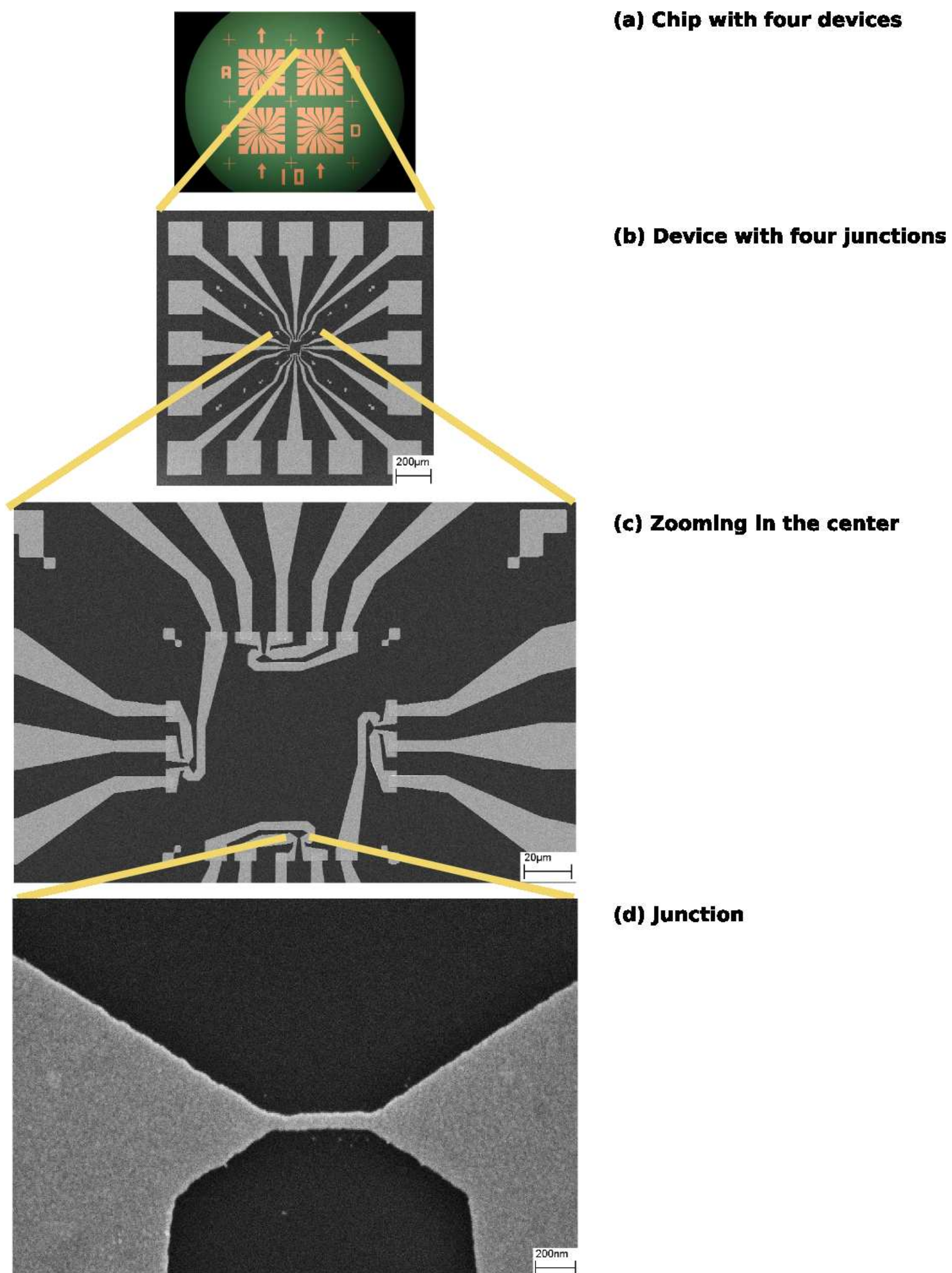

Figure 2.5: (a) A chip with four devices. (b) A device with four junctions, and 16 connectors for the four point measurement. (c) Center of a device. (d) A single junction with wire geometry. *Note that the lead design in (a) is not the same as in the other pictures.*

Chapter 3

Results

To study EM, a set of 30 junctions were migrated and the data analysed. First the measured conductance in electromigrated gold nanowires is presented, follwed by a discussion of the gap sizes and the obtained yield. Finally we analyze the implemented feedback with the help of the Joule heating model and present some possible improvements.

3.1 Discretised Conductance

During the breaking process it is possible to see a conductance discretisation which is due to the size reduction at a point in the nanowire. Some conductance steps are visible in Fig. (3.1). This discretisation is visible at room temperature because there are only few atoms left in the junction, whose size reaches the Fermi wavelength of electrons in gold. The small fluctuations around $1.5G_0$ in Fig. (3.1) can be due to reorganization of the atoms within the junction, which modify their positions between the possible lattice structures [11]. Moreover, previous published work [13] have shown that below $5G_0$ the conductance can show plateaux, which can occur, at non-integer values.

To determine whether the discretised conductance observed in our devices is due to quantum effects, we carried out a statistical analysis, the result is shown in Fig. (3.2). In this plot 8 measurements with plateaux below $4G_0$ were added together, in each measurement a fixed serie resistance was subtracted. We see that this statistics does not show conductance plateaux at exact integer numbers, which could be a result of the small number of measured junctions [6] or of the approximation for the series resistance, which can slightly change, depending on the geometry and the size of the junctions. But there are indications of quantization, firstly the distance between the

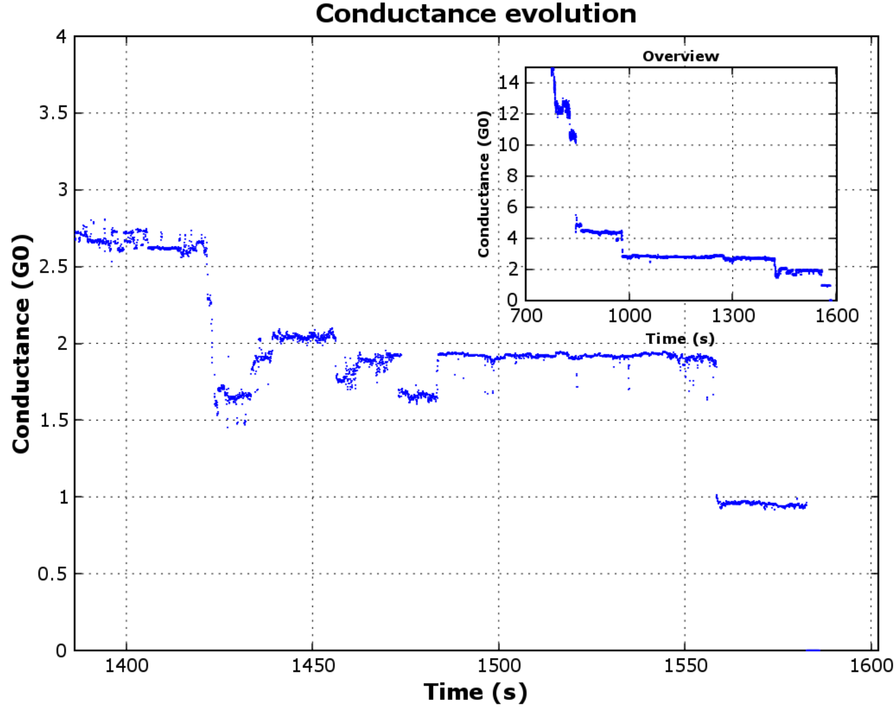

Figure 3.1: Quantization of the conductance during the breaking process of a junction. The inset shows a longer time interval. The fluctuations around $1.5G_0$ can be due to reorganization of the atoms within the junction.

peaks is almost constant and is in the order of $1G_0$ as shown with the black arrows in Fig. (3.2), moreover there is no value below $1G_0$ what could say that this is the last possible state of a quantized system.

The much smaller peaks at 1 and $2G_0$ than at $3G_0$ or more can be due to a stability problem of the atomic configuration on the two last plateaux tending to break before any measurement were performed. Moreover some atomic arrangements do not allow a $1G_0$ step but go from $2G_0$ directly to the tunneling regime [11].

3.2 Electromigration process

The electromigration can be observed in many ways such as conductance-voltage, current-voltage, conductance-time,... The IV-response of a nanowire during the whole process is plotted in figure 3.3. From point A to B the linear response follows Ohm's law $U = RI$, then at point B the EM starts increasing

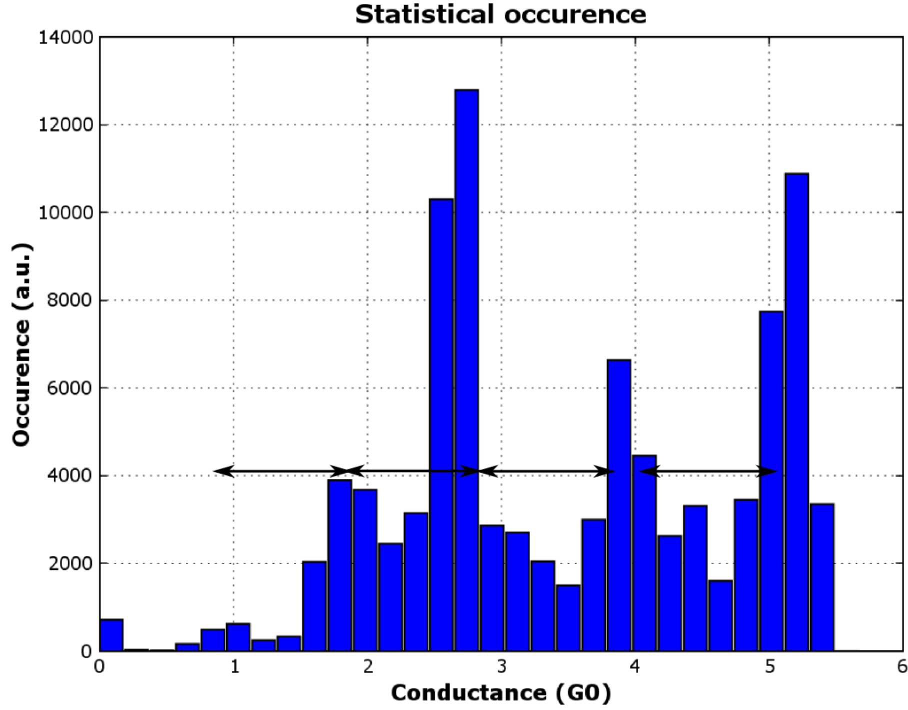

Figure 3.2: Occurrence statistics of the conductance measurement with a bin size of $0.1875G_0$. This plot show the occurrence of the conductance value taken from 8 electromigrated devices which showed value below $5G_0$. We see that the peaks are separated approximately by the same value, this is represented by the black arrows which are all of the same length. The non-integer value of the peaks can be due to our approximation for the series resistance, and to the low number of measured junctions [6]. The smaller peaks below $3G_0$ can arise from instability of the atomic configuration and from the fact that some atomic arrangements do not allow $1G_0$ [11].

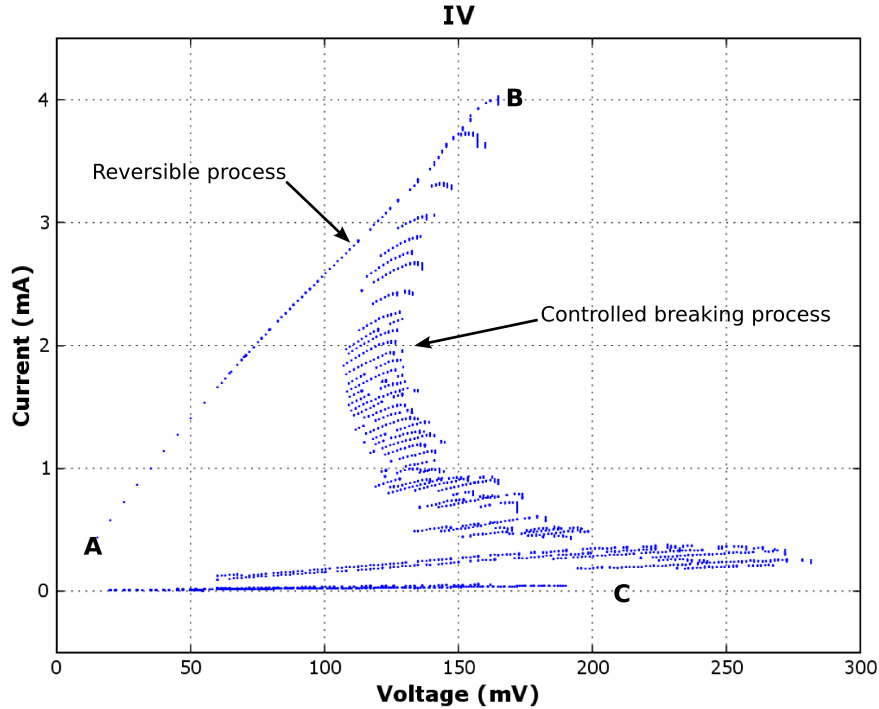

Figure 3.3: I-V curve of a whole nanowire EM: from A to B ohmic response, at point B start of EM increasing the resistance of the junction. The process evolves up to point C where the wire breaks. Between B and C the feedback mechanism is active, stepping down the voltage if the resistance (conductance) crosses a certain threshold.

the resistance of the junction. Between B and C the oscillations are produced by the feedback mechanism, which steps down the voltage each times changes in the resistance or the conductance over a certain threshold are detected. At point C the wire breaks, and the program stops the measurement.

3.3 Gap size

Evaluation of SEM picture showed that 7 junctions have gap sizes below 10 nanometers, 5 others between 10 and 20 nm, corresponding respectively to yields of 23% and 17% of the measured junctions. The rest of the junctions had a bigger size or were destroyed during the electromigration or the handling. Below 10 nm the resolution of the SEM pictures does not allow precise measurement, thus we were only able to set a upper bound for the gap size.

Size	Number	Yield*
< 10 nm	7	23%
$10 - 20$ nm	5	17%
$20 - 50$ nm	1	7%

Table 3.1: Size of the gaps approximated from SEM pictures. *Against the number of electromigrated junctions, not against the total number of fabricated junctions.

Figures (3.4) and (3.5) show broken junctions with gaps smaller than 10 nm as well as the resolution of the SEM images.

The low yields can be due to many problems. Firstly the lack of images resolution could lead to an overestimation of the gap sizes. Then as shown in Fig. (3.5), the EM starts in different locations along the junction and, if the starting points are very close together, the resulting end size can be the sum of the two voids. It is possible as well that our feedback algorithm is slow in detecting the break point (between 0.1 to 1 second) with respect to the atomic time scale. Therefore it is still applying a voltage after the gap has formed increasing gap sizes by giving energy to the atoms at the surface of the void. The atoms at the surface are weakly bound and therefore move easily, as well as preferring a stable atomic arrangement. This tends to replace spikes by smoother surface, increasing the gap size. A third possibility is that the heat production just before gap formation can be large enough to evaporate the atoms at the failure point.

In conclusion we could say that a more rapid detection of the breaking point is required by taking into account, in the last steps, every fluctuation of the junction resistance and not the averaged value. Another possibility is to apply only a constant voltage on the two last plateaus, instead of slowly increasing voltage ramps.

3.4 Critical Power

One can use the Joule heating model (see 1.4) to find the critical power P^* that must be dissipated in the junction for electromigration to start. As discussed in Chap. 1.4 the critical voltage is given by:

$$v^* = \sqrt{\frac{P^*}{G(1 - GR_s)}}. \tag{3.1}$$

We can assume that the series resistance R_s is approximately the resistance at the beginning when there is no void in the wire. The single fitting parameter

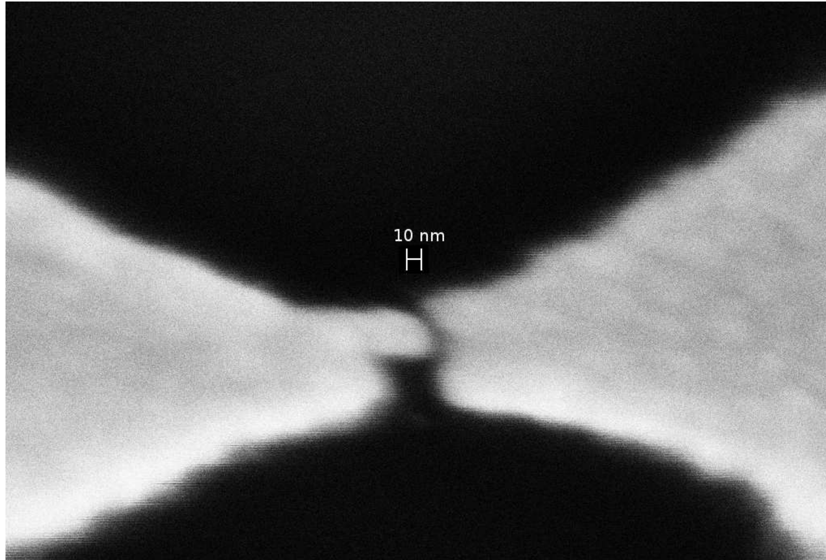

Figure 3.4: A broken junction of less than 10 nm.

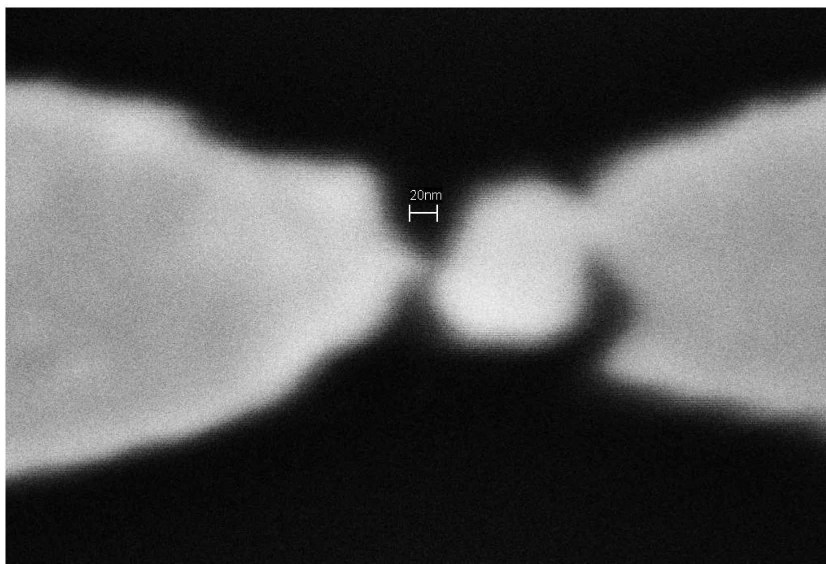

Figure 3.5: A broken junction of less than 10 nm, this picture show that the EM can start in two different locations.

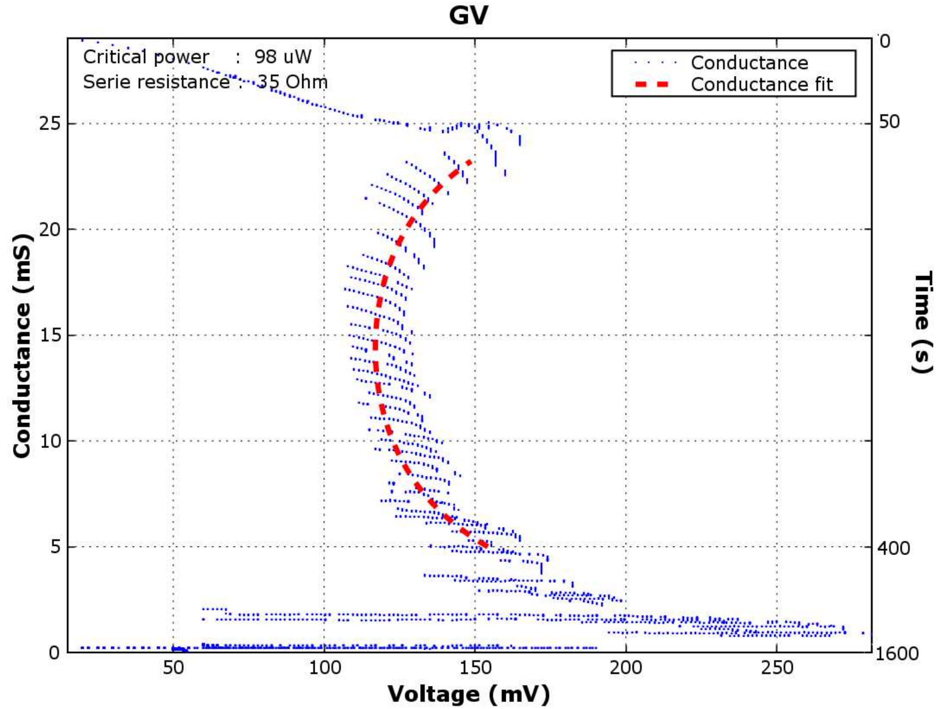

Figure 3.6: Plot of the conductance versus the voltage (dots), with a critical power fit (dashed line) according to the Joule heating model. The model is only valid to a limit of 2 mS, where the electron transport starts leaving the diffusion regime.

is therefore the critical power which was computed with a leastsquare fitting algorithm. A representative result is shown in figure 3.6, the dots represent the measured values, and the dashed line shows the fitted equation 3.1.

The values found with this fitting method are all of the same order of magnitude, but even if we take into account the different cross sections of the wires, the average critical power has a quite big standard deviation (see table 3.4). An explanation for this big deviation could be that our feedback mechanism does not really detect the electromigration but only prevents it from accelerating, meaning that the algorithm does not step down the voltage at the power at which the migration starts. A related error source is to use the entire data set instead of the external points where the EM occurs, this is creating a dependence of the critical power on the parameters of the feedback algorithm, like the starting value for the new voltage ramps. In our calculation all the points with a lower voltage in the conductance-voltage

Geometry	**Mean critical power (μW)**	**Standard deviation (μW)**
Wire	147	27
Bowtie	158	42

Table 3.2: Fitted critical power with standard deviation.

curve influence the leastsquare fitting algorithm.

Another problem arises from our approximation of the series resistance which can be slightly changed by the heat production within the leads. Moreover some physical difference of the junctions could explain the deviation, for example the thermal contact between the junction and the substrate is depending on the fabrication process. Therefore the power dissipation will be quite different leading to varying probe temperature during the breaking process and therefore to higher deviation in the measured critical power.

In order to get more accurate value we could try to evaluate the data differently, for example by giving more weight to the points at wich the algorithm steps down the voltage.

3.5 Feedback Algorithm

The low size yields (see 3.3) and the large critical power standard deviation (see 3.4) for the 30 measured junctions showed that the implemented algorithm is not yet optimal. Moreover it seems that the reaction time of the feedback at the breaking point is too long, increasing the void size after the break. But our feedback seems to be able to prevent the acceleration of the process such that the breaking occur in a controlled fashion as shown in Fig. (3.7). In this plot we see that big changes in the conductance are followed by the stepping down of the voltage. We can conclude that our feedback get enough informations about the EM evolution by measuring only the resistance or conductance evolution, but it seems in Fig. (3.7) to be quite conservative with the choosen limit, staying a long time on the same conductance plateau because of the built-in voltage limit. We could try to give higher limits to accelerate the process.

The first chip was measured with the normalized breaking rate $\frac{1}{R}\frac{\partial R}{\partial t}$ feedback, but it showed that this value is too noisy (Fig. 3.8) to be used as a good feedback mechanism. The threshold value needed constantly to be manually adjusted, to avoid many steps down of the voltage. The noise could arise from small physical variation of the resistance due to thermal noise or shot noise, or to fluctuations during the measurement. We quickly changed this part of the algorithm to use the conductance feedback.

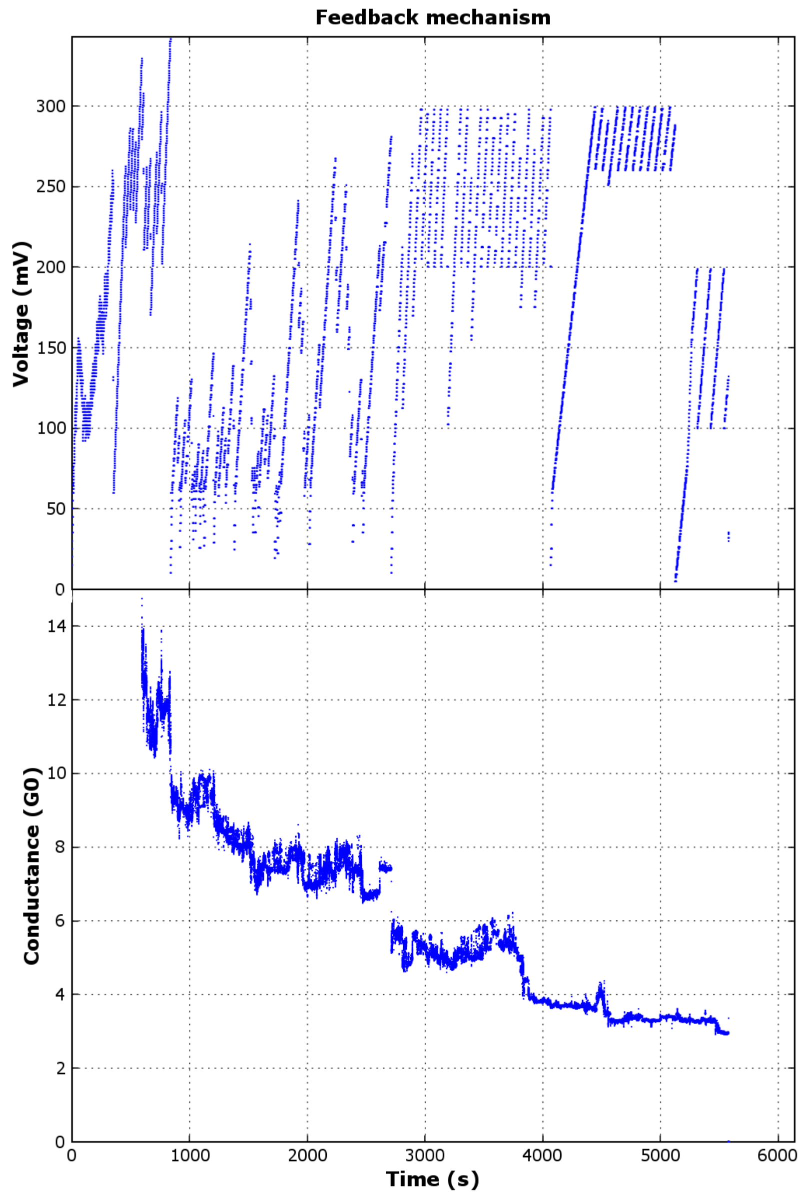

Figure 3.7: The feedback mechanism in action. Between 0 and 800 s the algorithm is using the resistance feedback, then only the conductance feedback is used. We see in the middle of the plot that during a long time, because only slow changes in the conductance append, the only limit is the maximal voltage at 300 mV. At 4500 s the peak is well detected by the feedback, which start a new voltage ramp from a lower voltage. The big voltage jumps at about 4000 and 5000 s are due to a manual changes in the feedback parameters, all the other voltage changes are driven automatically by the feedback mechanism.

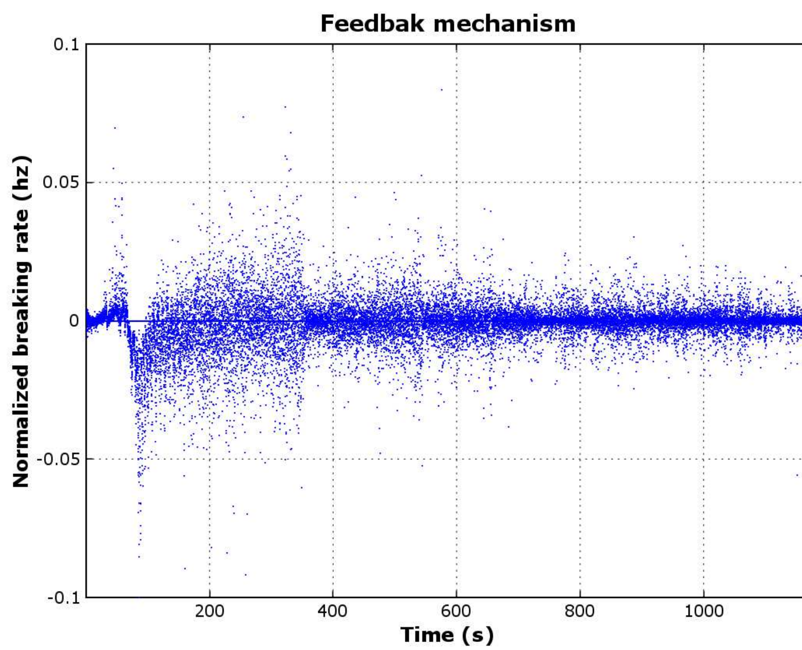

Figure 3.8: Plot of the normalized breaking rate. This plot shows the randomness of the computed value for $\frac{1}{R}\frac{\partial R}{\partial t}$, which could arise from fluctuation in the resistance measurement and to the small time interval dt.

Chapter 4

Outlook

The next step is to improve the feedback mechanism by fine tuning the parameters in order to increase its production yields of nanometer-spaced junctions. Moreover by allowing more larger changes in the conductance during the first part of the conductance feedback, it would be possible to accelerate the whole process. It would also be possible to add new EM detection with for example using the power or a measure of the local temperature [10].

Another technique to determine the gap size would be to use the John G. Simmons formula [7]. This calculation allows one to find the gap size by using the end resistance, but it needs the work function for electrons in gold on top of a silicon oxide substrate. Thus this value should be measured. A second problem arises from the unknown area which contributes to the tunneling process, a good approximation has to be found, perhaps by looking at higher resolution SEM pictures.

In order to increase the accuracy and the bandwith of the resistance measurement we could include the junction in an LC-circuit. Then by applying an AC voltage and looking for the resonance frequency of the resulting RLC-circuit, we can obtain the junction resistance.

An other idea to accelerate the process could be to compare junctions broken with a single voltage ramp [3] to junctions broken with an active feedback mechanism. One junction was electromigrated following this idea and produced the same characteristic as the normally broken junctions. It is promising, but without more tests, it is not possible to make any conclusion.

Chapter 5

Conclusion

During this work we were able to control EM of gold nanowires at room temperature using different feedback mechanisms. We have observed discretised conductance, and showed that below 5 G_0 there are indications of quantization. Statistics showed that 23% of the produced gaps were bellow 10 nm, this yield are promising but need to be increased by fine tuning the feedback algorithm in order to use the junctions for molecular electronics. Then we proposed some possible improvements of the algorithm, for example by allowing bigger changes at the beginig of the conductance feedback to accelerate the process. Moreover it is needed to reduce the reaction time at the breaking point to avoid increasing the size after the break.

5.1 Acknowledgements

I want to thank a lot Prof. Dr. Wallraff Andreas, Dr. Leek Peter, and Puebla Gabriel for giving me the possibility to do this semester work in the Quantum Device Lab at ETH Zurich and for their help.

Appendix A

Encountered problems

A.1 Electrostatic

We did not ground the pins of the chips for the first set of devices, this leads to many unwanted broken junction due to probable charging/discharging on the bottom of the plastic box, or due to the handling without an anti static band. We have then grounded everything avoiding quite all the unwanted effects of electrostatic charges, but some broken junction remain unexplained. A possible problem can be the electrostatic charges in the surrounding air, to remove these charges an ionization fan can be used.

A.2 Fabrication

There were many issues during the fabrication process, which led to increased time for sample fabrication and larger time intervals between measurements. Common problems are shown in pictures A.1 and A.2. These are lift off problems, the metal did not stay on the substrate, and was partially or totally removed with the photoresist.

Furthermore the bonding wires seemed to be very difficult to fix to the contact pads on the devices. But it was found that if the surface is cleaned with acetone in a ultrasonic bath, wire bonding requires less effort.

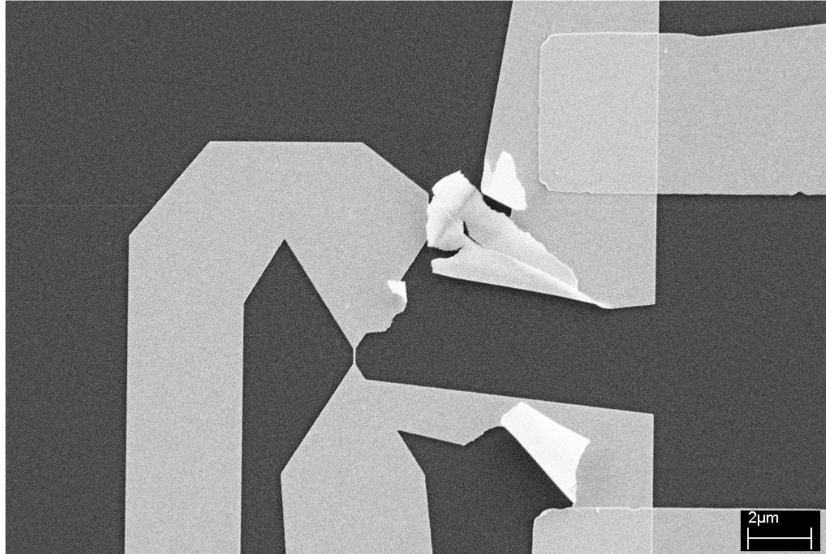

Figure A.1: A problem during the lift off, the metal did not stay on the substrate and got folded.

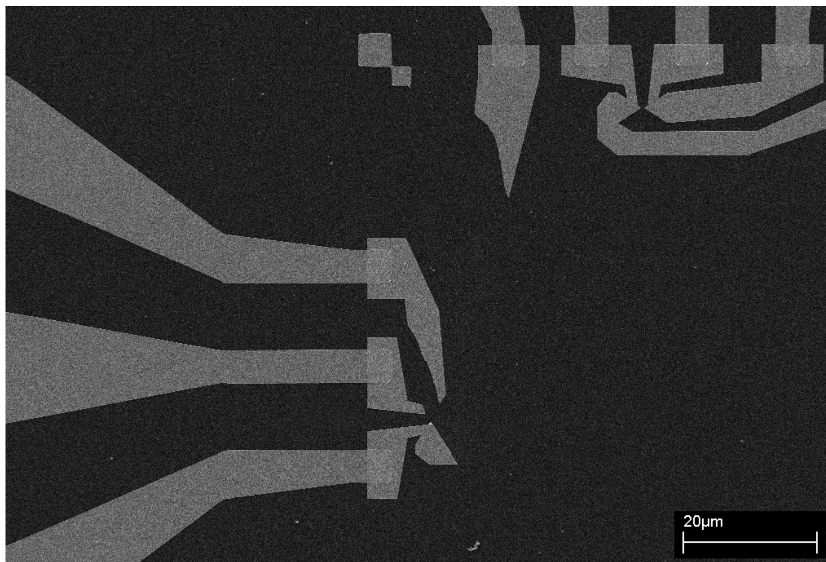

Figure A.2: An other problem during the fabrication, some parts of metal were removed with the photoresist.

List of Figures

1.1 Schematic EM Mass flux . . . 2
1.2 EM Forces on a metallic ion . . . 3
1.3 Diffusion locations . . . 5
1.4 Breaking mechanism . . . 6
1.5 A melted junction . . . 6
1.6 Wire Schematic . . . 9
1.7 Breaking phases . . . 10

2.1 Leads design 1 . . . 13
2.2 4 point measurement . . . 14
2.3 Leads design 1 . . . 16
2.4 Leads design 2 . . . 16
2.5 Device overview on different scales . . . 18

3.1 Quantization of the conductance . . . 20
3.2 Conductance quantization statistics . . . 21
3.3 I-V curve . . . 22
3.4 A broken junction . . . 24
3.5 An other broken junction . . . 24
3.6 Critical power fit . . . 25
3.7 Feedback mechanism . . . 27
3.8 Normalized breaking rate . . . 28

A.1 Fabrication problem . . . 32
A.2 Fabrication problem . . . 32

List of Tables

2.1 Devices sizes 17

3.1 Gaps sizes 23
3.2 Critical power 26

Bibliography

[1] Black J.R. Metalization Failures In Integrated Circuits, *RADC Technical Report*, Vol. TR-68-243, October 1968.

[2] Koetter T. Gefuegeeinfluss auf das Elektormigrationsverhalten von Kupferleitbahnen fuer hoechstintegrierte Schaltungen, Thesis, TU Dresden

[3] Trouwbrost M.L., et al. The role of Joule heating in the formation of nanogaps by electromigration, *arXiv*, cond/mat v4 13 Jul. 2006

[4] Lloyd J.R., Electromigration for Designers: An Introduction for the Non-Specialist, TechOnline

[5] Crowell B.W., Quantized Conductance of a Gold Nanowire Break Junction, Georgia Institue of Technology, Atlanta

[6] Muller C.J., Quantization effects in the conductance of metallic contacts at room temperature, *Phys. Rev. B*, Vol. 53, N 3, January 1996

[7] Simmons J.G., Generalized Formula for the Electric Tunnel Effect between Similar Electrodes Separated by a thin Insulating Film, *J. Appl. Phys.*, Vol. 34, N 6, June 1963

[8] Strachan D.R. et al., Controlled fabrication of nanogaps in ambient environement for molecular electronics, *App. Phys. Lett.*, Vol 86, 2005

[9] Hongkung P. et al., Fabrication of metallic electrodes with nanometer separation by electromigration, *Appl Phys. Lett.*, Vol 75, 2, 1999

[10] Esen G. and Fuhrer M.S., Temperature control of electromigration to form gold nanogap junctions, *Appl. Phys. Lett.*, Vol 87, 2005

[11] Rodrigues V. et al., Signature of Atomic Structure in the Quantum Conductance of Gold Nanowires, *Phys. Rev. Lett.*, Vol 85, 19, 2000

[12] Liddle J.A. et al., Resist Requirements and Limitations for Nanoscale Electron-Beam Patterning, *Mat. Res. Soc. Symp. Proc.* 739 (19): 19-30, 2003

[13] de Heer W.A. et al., Fractional quantum conductance in Gold nanowires, *Zeitschrift fr Phys. B Cond. Mat.*, Vol. 104, 3, 1997

[14] Krans J.M et al., *Nature*, The signature of conductance quantization in metallic point contacts, Vol. 375, 1995

[15] Ihn T., Manuscript for the lectures *H*albleiter-Nanostrukturen, ETH Zürich, 2005

[16] Datta S. et al., *Phys. Rev. B*, Vol.79, 1997

[17] Cui X. D. et al., *Science*, Vol. 294, 571 2001

[18] Xiao X. Y. et al., *Nano Lett.*, Vol. 4, 267 2004

[19] Wikipedia